



ARTICLE

# Preparation and Study of Borosilicate Foam Glass with High Thermal Insulation and Mechanical Strength

Yiwen Zhang<sup>1</sup>, Jianjun Xie<sup>1,\*</sup>, Minghui Sun<sup>1</sup>, Shaolong Wang<sup>1</sup>, Tengfei Xu<sup>2,3</sup>, Yonggen Xu<sup>2,3</sup>, Xiaoqing Ding<sup>2,3</sup>, Ying Shi<sup>1</sup> and Lei Zhang<sup>1</sup>

<sup>1</sup>School of Material Science and Engineering, Shanghai University, Shanghai, China

<sup>2</sup>Huichang New Material Co., Ltd., Xuancheng, China

<sup>3</sup>Changda Thermal Insulation Technology Co., Ltd., Xuancheng, China

\*Corresponding Author: Jianjun Xie. Email: xiejianjun@shu.edu.cn

Received: 23 June 2022 Accepted: 29 July 2022

## ABSTRACT

Foam glass is a kind of green building material that is widely used because of its excellent thermal insulation and mechanical properties. In this study, the borosilicate foam glass was fabricated by powder sintering method using recycled soda lime waste glass, quartz, and borax as the primary raw materials.  $\text{CaCO}_3$  was used as a foaming agent and  $\text{Na}_2\text{CO}_3$  as a flux agent. Results showed that as the quartz content decreases from 30 to 17.5 wt.% and borax content increases from 5 to 17.5 wt.%, the pore size, porosity, and thermal insulation of borosilicate foam glass increase significantly, while the compressive strength decreases slightly. When the content of quartz and borax are both 17.5 wt.%, borosilicate foam glass with outstanding performance can be prepared, whose pore distribution is uniform, mean pore size is 1.93 mm, total porosity is 83.44%, thermal conductivity is 0.0711 W/(m·K), and compressive strength is 2.37 MPa. Finally, the influences of foaming agent content, flux agent content, foaming temperature, and holding time on the pore structure and various properties of borosilicate foam glass were investigated by orthogonal test. According to the results, the foaming temperature has a significant effect, and appropriate foaming agent content, flux agent content, and holding time help to form a uniform pore structure, thereby improving the thermal insulation and mechanical strength of the borosilicate foam glass.

## KEYWORDS

Foam glass; waste glass; thermal conductivity; compressive strength

## 1 Introduction

Foam glass is a kind of artificial light porous material whose pores account for 50%–90% of the total volume, pore size is between 0.5–5 mm, and bulk density is generally 0.1–0.5 g/cm<sup>3</sup>. Depending on the production method, its pores can be divided into independent closed pores and connected open pores, and they can be suitable for thermal and acoustic insulation, respectively [1–3]. Benefiting from the unique structure of uniform distribution of glass phase and gas phase in foam glass, it exhibits many advantages over other traditional thermal insulation materials (organic foam and mineral wool, etc.), such as attractive thermal insulation and thermal stability, high mechanical strength, resistance to humidity and water, non-combustibility, and non-toxicity [4–6]. In addition, foam glass has a much longer lifespan than



traditional thermal insulation materials due to its excellent chemical stability [2]. Since Saint-Gobain successfully developed foam glass in the 1930s [6], this kind of green and environmentally friendly material with excellent performance has been widely used in building materials, the petrochemical industry, and other fields. At the same time, it has vast potential application value in biological filtration and medical equipment (bioactive glass-ceramics for bone tissue application) [4,7].

Currently, most foam glass produced and sold in the market is mainly made of recycled waste glass, such as flat glass, bottle glass, bulb glass, and other ordinary soda lime glass with low softening points [8–13]. Besides, solid wastes containing the glass phase can also be used as raw materials, such as cathode ray tube (CRT) glass, fly ash, and mineral waste [14–19]. These raw materials are mixed with a foaming agent, flux agent, and other additives, and then the foam glass products can be obtained through preheating, sintering, foaming, annealing, and other processes [4,5]. At high temperatures, the foaming agent releases gas by decomposition or oxidation reaction inside the softened mix, and a stable porous structure can be achieved after complete cooling [12]. This method, known as the powder sintering method, is the most commonly used method to prepare foam glass in industrial production and scientific research [4]. Foam glass can not only meet the needs of specific functions of porous materials but also solve the problem of solid waste treatment, which has significant practical and economic benefits [9].

Compared with ordinary soda lime foam glass, borosilicate foam glass has more outstanding properties, such as uniform pore distribution, strong acid and corrosion resistance, higher mechanical strength, and lower coefficient of thermal expansion [20]. This is because boron atoms can exist in the form of  $[\text{BO}_4]$  tetrahedron and connect with  $[\text{SiO}_4]$  tetrahedron, which increases the integrity and compactness of the glass network structure. Wang et al. [21,22] prepared a high-temperature resistant adhesive with high bonding strength that can join zirconia with nickel-based superalloys by introducing borosilicate glass. The experimental results proved the above mechanism. Therefore, many scholars have studied this kind of foam glass. Zhai et al. [23–25] used pure chemical reagents as raw materials to study the effects of  $\text{CaCO}_3$ ,  $\text{MnO}_2$ , and carbon black as foaming agents, respectively. They clarified the foaming mechanism through molecular dynamics simulation. However, pure chemical materials have the problem of high cost. Taurino et al. [26] used waste borosilicate glass dismantled from a washing machine as raw material to prepare foam glass-ceramic with high mechanical strength. They studied the effect of foaming temperature on the sinter-crystallization ability. Chinnam et al. [27] studied the fabrication of foam glass using pharmaceutical waste-derived borosilicate glass without adding an external foaming agent. They found that foaming ability depended on the initial powder particle size. This research has a particular frontier. Salleh et al. [28,29] prepared borosilicate foam glass with a low thermal expansion coefficient by mixing and sintering borosilicate glass and hollow glass microspheres with vinyl ester resin. The study results show that the thermal expansion coefficient decreases with increasing hollow glass microsphere content at the measurement temperature from  $30^\circ\text{C}$  to  $70^\circ\text{C}$ . Erasmus et al. [7] used  $\text{NH}_4\text{HCO}_3$  as a foaming agent to sinter borosilicate glass, borophosphate glass, and phosphate glass into foam glass as a bioactive scaffold. The obtained foam glass was immersed in simulated body fluid to assess the dissolution, and then its mechanical properties, microstructure, and crystallization were analyzed.

However, there are few reports on the thermal insulation and mechanical strength of borosilicate foam glass simultaneously. Accordingly, this paper aims to prepare borosilicate foam glass with high thermal insulation and mechanical strength, which can be used as insulation materials in buildings and infrastructures to reduce energy consumption and greenhouse gas emission. First, by adding quartz and borax to the recycled soda lime waste glass to adjust the content of  $\text{SiO}_2$  and  $\text{B}_2\text{O}_3$ , and adding a small amount of feldspar powder and dolomite powder to supplement the alkali metal and alkali earth metal elements, through high temperature molten and water quenching to obtain special borosilicate parent glass. Then, borosilicate parent glass was used as raw materials with  $\text{CaCO}_3$  as foaming agent and  $\text{Na}_2\text{CO}_3$  as flux agent to prepare borosilicate foam glass by powder sintering method. As shown in

**Table 1**, six borosilicate parent glass formulations and additives contents were designed so that the proportions of quartz and borax were 6:1, 4:1, 2:1, 1:1, 1:2, and 1:4, respectively. Finally, based on determining the best ratio of quartz and borax, an orthogonal test was designed with foaming agent content, flux agent content, foaming temperature, and holding time as the main factors. Properties such as pore size, bulk density, total porosity, thermal conductivity, and compressive strength were carried out to assess the performance of the developed borosilicate foam glass. In this study, the waste glass resources were effectively utilized, and borosilicate foam glass with prominent comprehensive properties was prepared, which provided a theoretical basis and reference for the scientific research and production of borosilicate foam glass.

**Table 1:** Content of raw materials in each formulation (wt.%)

Sample	Quartz	Borax	Soda lime glass	Feldspar powder	Dolomite powder	Foaming agent	Flux agent
A	30	5	55	5	5	3	3
B	28	7	55	5	5	3	3
C	23.33	11.67	55	5	5	3	3
D	17.5	17.5	55	5	5	3	3
E	11.67	23.33	55	5	5	3	3
F	7	28	55	5	5	3	3

## 2 Experimental and Characterization

### 2.1 Raw Materials

The raw materials such as quartz, borax, and recycled soda lime waste glass used in the experiment were all from Changda Thermal Insulation Technology Co., Ltd. (China) and their chemical compositions are shown in **Table 2**.  $\text{CaCO}_3$  (CP, Sinopharm) and  $\text{Na}_2\text{CO}_3$  (CP, Sinopharm) were used as foaming agents and flux agents, respectively.

**Table 2:** Chemical composition of raw materials (wt.%)

Raw materials	$\text{SiO}_2$	$\text{CaO}$	$\text{Na}_2\text{O}$	$\text{Al}_2\text{O}_3$	$\text{Fe}_2\text{O}_3$	$\text{MgO}$	$\text{K}_2\text{O}$	$\text{B}_2\text{O}_3$
Quartz	95.25	0.31	0	2.25	2.18	0	0	0
Borax	0	0	29.83	0	0	0	0	70.17
Soda lime glass	63.37	13.17	12.66	3.35	3.05	3.08	1.31	0
Feldspar powder	60.99	3.73	3.43	20.14	1.55	0.83	9.33	0
Dolomite powder	2.86	55.76	0	2.11	2.21	37.06	0	0

### 2.2 Experimental Procedure

The raw materials such as quartz, borax, and recycled soda lime waste glass are mixed according to the designed mass ratio (**Table 1**) and ball milled with ethanol in a planetary ball for 4 h at 250 rpm subsequently. After drying, the mixtures were placed in a corundum crucible and put into a muffle furnace for melting. Heating at 5 °C/min from room temperature to 1200°C and holding for 60 min, water quenching to obtain borosilicate parent glass at last.

The borosilicate parent glass was ball milled into powder and mixed with a certain amount of  $\text{CaCO}_3$  and  $\text{Na}_2\text{CO}_3$  in a ball mill for 4 h at 250 rpm. The dry mixtures were loaded in a stainless steel mold pre-sprayed with a release agent and sintered according to the preset program. Heated from room temperature to  $400^\circ\text{C}$  at the rate of  $5^\circ\text{C}/\text{min}$  and held for 20 min to remove the moisture in mixtures. Then raised to a foaming temperature at  $10^\circ\text{C}/\text{min}$  and held for a period to complete the foaming procedure. Subsequently, it cooled down to  $600^\circ\text{C}$  at  $10^\circ\text{C}/\text{min}$  and held for 20 min to anneal. Finally, cool down to room temperature by natural cooling. The borosilicate foam glass was processed into a block sample of  $30 \times 30 \times 30 \text{ mm}^3$  for characterization and test. The main experimental procedure is shown in Fig. 1.

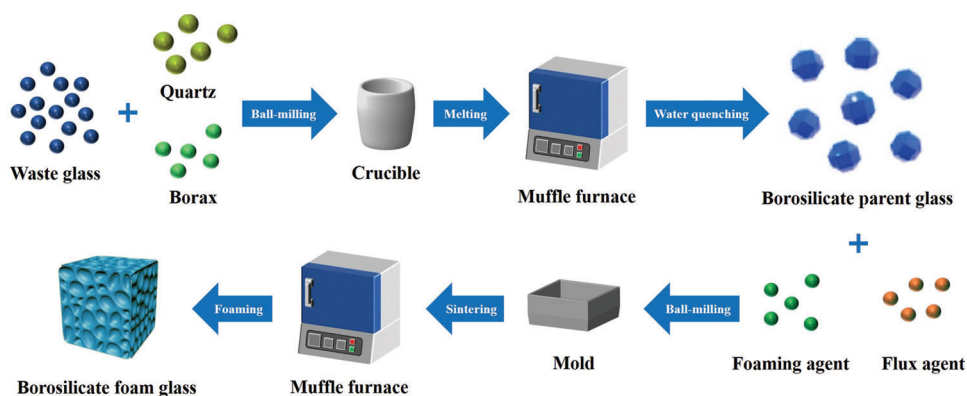


**Figure 1:** Experimental procedure of borosilicate foam glass preparation

After the optimal ratio of quartz and borax was determined, porosity size, water absorption, thermal conductivity, and compressive strength were taken as performance indexes, and the foaming agent content, flux agent content, foaming temperature, and holding time were selected as influencing factors. Three levels were selected for each factor, and the orthogonal tests were conducted according to  $L_9(3^4)$ . The design of the orthogonal test is shown in Table 3.

**Table 3:** Orthogonal test schedule

Level	W/foaming agent content (wt.%)	X/flux agent content (wt.%)	Y/foaming temperature ( $^\circ\text{C}$ )	Z/holding time (min)
1	1	1	750	15
2	3	3	800	30
3	5	5	850	45

### 2.3 Characterization Methods

Differential scanning calorimetry (DSC) was used to detect any endothermic or exothermic responses during the preparation of borosilicate parent glass (STA 449 F3, NETZSCH, Germany) and to determine its glass transition temperature  $T_g$  and softening temperature  $T_s$ . The FT-IR spectra of the borosilicate parent glass were recorded at room temperature using KBr disc technique (Nicolet Nexus FT-IR, Thermo, USA). High-temperature viscosity between  $600^\circ\text{C}$ – $1200^\circ\text{C}$  was obtained by using a rotation viscometer (RSV 1600, Orton, USA). The micromorphology of the borosilicate foam glass samples was examined using a scanning electron microscope (GeminiSEM 300, ZEISS, Germany), and the mean pore size and pore size distribution were calculated by the analysis software Nano Measurer. X-ray diffraction (XRD) analysis was performed with a scanning range of  $10^\circ$  to  $90^\circ$  and a scanning speed of  $5^\circ/\text{min}$  (3KW D/MAX2200V PC,

Riken Electric, Japan). The compressive strength of the borosilicate foam glass samples was measured with a universal material testing machine (JWE-50, China). The thermal conductivity of the borosilicate foam glass samples at room temperature was measured using the transient hot line method (TC3000E, XIATECH, China). The bulk density, total porosity, and water absorption of the borosilicate foam glass samples were calculated using the equation [13,14,23–25]:

$$\rho = \frac{m_0}{V} \quad (1)$$

$$\varepsilon = \frac{\rho_0 - \rho}{\rho_0} \times 100\% \quad (2)$$

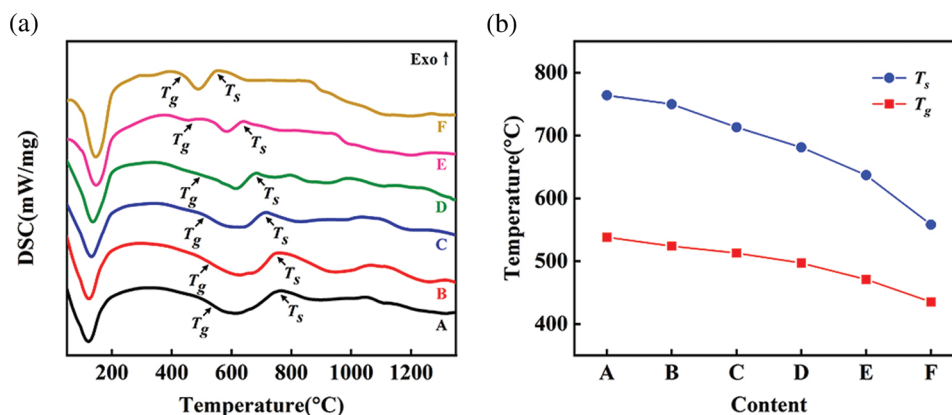
$$w = \frac{m_1 - m_0}{V \times \rho_w} \times 100\% \quad (3)$$

where  $\rho$ ,  $\varepsilon$ , and  $w$  are the bulk density ( $\text{g/cm}^3$ ), total porosity (%), and water absorption (%) respectively,  $m_0$  and  $m_1$  are the dry weight and wet weight in units of a gram, respectively,  $V$  is the volume of the borosilicate foam glass samples in units of  $\text{cm}^3$ ,  $\rho_0$  are the weight of the full ground and dried borosilicate foam glass samples without pores inside of a unit volume,  $\rho_w$  is the density of deionized water, whose value is  $1 \text{ g/cm}^3$ .

### 3 Results and Discussion

#### 3.1 Effects of Quartz and Borax Content on Borosilicate Parent Glass

Fig. 2 shows the DSC curve and variation trend of  $T_g$  and  $T_s$  of borosilicate parent glass. A significant endothermic peak is seen in the range of  $100^\circ\text{C}$ – $200^\circ\text{C}$ , which is mainly caused by the evaporation of water in raw materials (Fig. 2a). As the content of quartz decreases and the content of borax increases, the  $T_g$  and  $T_s$  of borosilicate parent glass gradually decrease, and it is found that the  $T_s$  of each content is lower than  $800^\circ\text{C}$  (Fig. 2b). According to literature reports,  $\text{CaCO}_3$  begins to decompose into  $\text{CO}_2$  at  $800^\circ\text{C}$  [30], it is suitable to choose  $\text{CaCO}_3$  as the foaming agent. After the temperature exceeds  $1100^\circ\text{C}$ , the DSC curve declines continuously, which is the result of borosilicate parent glass continuing to absorb heat in the molten liquid phase state.

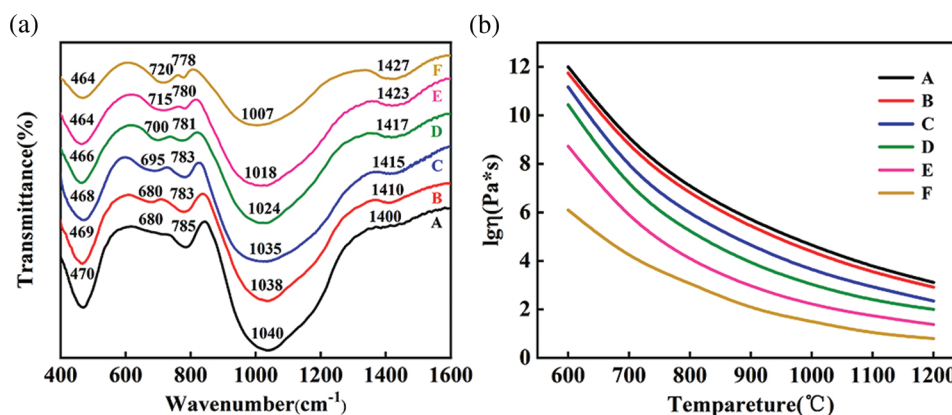


**Figure 2:** DSC curve (a) and variation trend of  $T_g$  and  $T_s$  (b) of borosilicate parent glass

The wavenumber and assignment of FT-IR spectra of borosilicate parent glass are presented in Table 4 [31–33], and the FT-IR spectra are shown in Fig. 3a.  $460 \text{ cm}^{-1}$  is attributed to bending vibration of Si-O-Si, and the vibration intensity is larger, which indicates that Si-O-Si is abundant. With the quartz content decreasing and borax content increasing, the bending vibration gradually shifted to lower wavenumbers, and the vibration intensity gradually decreased, indicating that the amount of  $[\text{SiO}_4]$  decreased.  $780 \text{ cm}^{-1}$  is attributed to the stretching vibration of O-Si-O.

**Table 4:** Assignment of FT-IR absorbance spectra of borosilicate parent glass

Wavenumber/cm <sup>-1</sup>	Assignment
460	Bending vibration of Si-O-Si
780	Stretching vibration of O-Si-O
1020–1060	Antisymmetric stretching vibration of Si-O-Si
940–1080	Antisymmetric stretching vibration of [BO <sub>4</sub> ]
1400	Antisymmetric stretching vibration of [BO <sub>3</sub> ]
700	Bending vibration of [BO <sub>3</sub> ]

**Figure 3:** FT-IR spectra (a) and variation trend of viscosity (b) of borosilicate parent glass

The appeared band near 700 cm<sup>-1</sup> is attributed to the bending vibration of [BO<sub>3</sub>], whose antisymmetric stretching vibration appears at 1400 cm<sup>-1</sup>. It can be seen that the amount of [BO<sub>3</sub>] is increasing. The appeared band near 1040 cm<sup>-1</sup> is the combination of antisymmetric stretching vibration of [SiO<sub>4</sub>] and [BO<sub>4</sub>]. It is reported that the two tetrahedral structures of [SiO<sub>4</sub>] and [BO<sub>4</sub>] are interconnected to enhance the glass structure [34,35]. The bending vibration at this position is weakened, which indicates that the amount of [SiO<sub>4</sub>] and [BO<sub>4</sub>] decreased.

The viscosity of borosilicate parent glass samples A–F at 600°C–1200°C is shown in Fig. 3b. It can be seen that with the decrease of quartz content and increase of borax content, the viscosity at the same temperature gradually decreases. There are two main reasons for this phenomenon [36,37]: (1) The Si-O bond, whose bond energy is intense, in the glass network structure are reduced as the content of quartz decreases, so the temperature required to melt the borosilicate parent glass is reduced. (2) The [BO<sub>3</sub>] triangle, floating in the voids of the glass structure, makes the structure loose and increases with the increase of borax content. These transitions destroy the structural integrity of the glass, thereby reducing the viscosity of borosilicate parent glass.

### 3.2 Effects of Quartz and Borax Content on Borosilicate Foam Glass

The borosilicate parent glass powder mixed with 3 wt.% CaCO<sub>3</sub> and 3 wt.% Na<sub>2</sub>CO<sub>3</sub>, and then hold at 800°C for 30 min. The obtained borosilicate foam glass is shown in Fig. 4. The pore structure of foam glass determines its performance, so the analysis of pore structure is fundamental. When the content of quartz is 30 wt.% and the content of borax is 5 wt.% (Fig. 4a), no apparent pores appear in the sample, and most pores are distributed in 0.2–0.5 mm. According to the DSC result (Fig. 2), the  $T_s$  of the borosilicate parent glass A is

764°C, and the viscosity of the melt is high at 800°C (Fig. 3b). The bubbles did not expand enough, resulting in a low foaming degree and small pore size of this borosilicate foam glass.

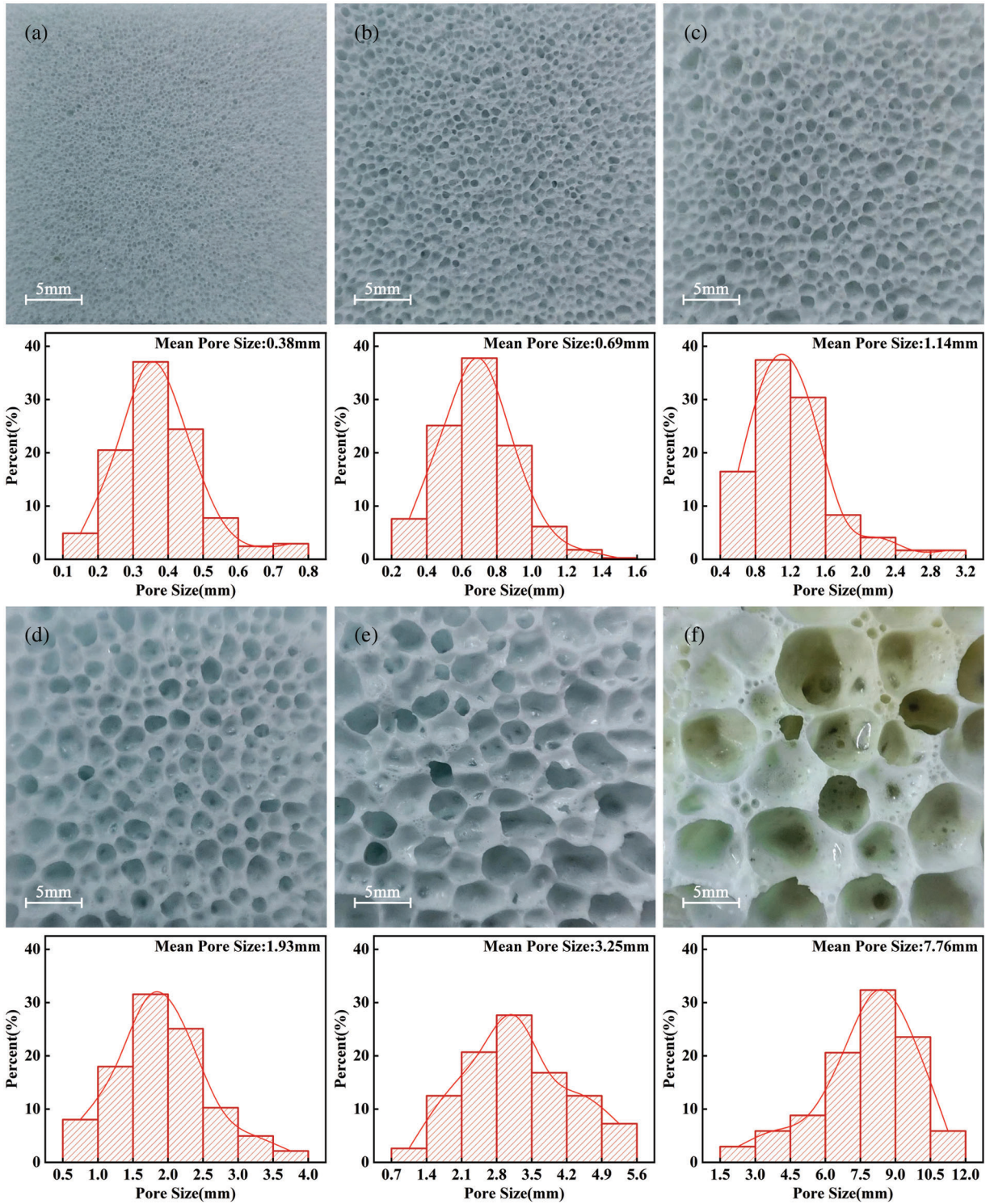


**Figure 4:** Optical photographs and pore size distribution of borosilicate foam glass ((a)–(f) are borosilicate foam glass foamed from borosilicate parent glass A–F, respectively)

The samples obtained by foaming with the borosilicate parent glass B-E formed an apparent independent closed pore structure (Figs. 4b–4e). Furthermore, it can be seen that the pore size gradually increases, and the pore size distribution moves in the direction of large size. This is because bubbles grow more easily as the viscosity of borosilicate parent glass decreases. The viscosity of borosilicate parent glass samples B–E at 800°C is between  $10^4$ – $10^{6.73}$  Pa·s (Fig. 3b), and its viscosity and gas pressure in the bubbles remain a relative balance, thus forming this kind of uniform and regular pore structure. This phenomenon is basically consistent with Petersen et al.'s view [38] that when metallic carbonate such as  $\text{CaCO}_3$  is used as a foaming agent, the optimal viscosity window is within  $10^4$ – $10^6$  Pa·s. Finally, the mean pore size increases to 7.76 mm (Fig. 4f). This is because the viscosity of borosilicate parent glass sample F is too low at 800°C (Fig. 3b), and bubbles are easier to expand under the same internal gas pressure conditions.

Fig. 5 is a scanning electron microscope photo of borosilicate foam glass samples, and it can be clearly observed that the inside of pores of each sample is relatively smooth. As quartz's content decreases and borax's content increases, the pore size gradually increases. In addition, it can be found that there are tiny pores at the connection of pores and on the pore walls. These tiny pores are regular in shape and exhibit a uniform circular structure, and this phenomenon can be explained by the mechanism of bubble growth in the glass melt. Méar et al. [39] believed that the process of bubble growth is similar to the model of grain coarsening. When the bubbles grow to a certain extent, the large bubbles grow by swallowing the smaller bubbles until they shrink or even disappear. At last, as the temperature decreases and the melt cools, the tiny pores that have not been swallowed are retained.

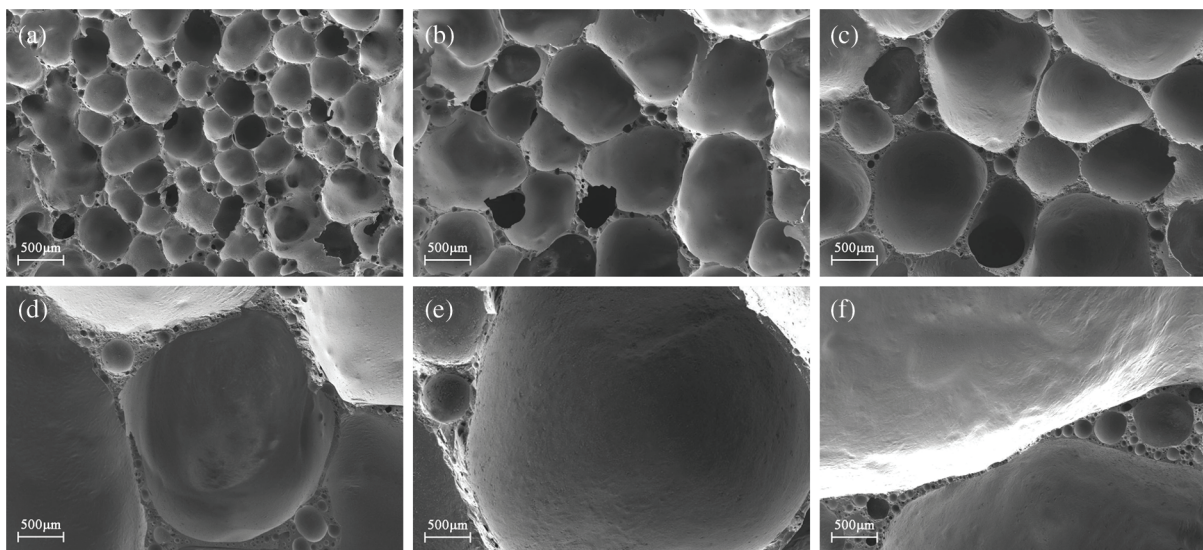


**Figure 5:** SEM micrographs of borosilicate foam glass ((a)–(f) are borosilicate foam glass foamed from borosilicate parent glass A–F, respectively, with the magnification of 25×)

Fig. 6 displays the XRD patterns of borosilicate foam glass samples, and all borosilicate foam glass samples display similar positions of the diffraction peaks. There are prominent steamed bread peaks in the diffraction range of  $20^\circ$ – $40^\circ$ , indicating a large amount of amorphous glass phase in borosilicate foam glass. By comparing standard PDF cards with MDI Jade software, it can be found that the main crystalline phase is wollastonite ( $\text{CaSiO}_3$ , PDF#72-2297), and the second crystalline phase is diopside ( $\text{CaMg}(\text{SiO}_3)_2$ , PDF#82-0599). The wollastonite crystalline phase is mainly precipitated by the reaction between CaO generated by the decomposition of  $\text{CaCO}_3$  and  $\text{SiO}_2$  in the glass phase [17,19,40]. With the decrease of quartz content and increase of borax content, the  $[\text{BO}_3]$  in borosilicate parent glass increases

and the glass structure gradually loosens, making it more likely for  $\text{Ca}^{2+}$  ions to react with  $\text{SiO}_2$  in the glass phase, thus enhancing the crystallization of wollastonite. Østergaard et al. [41] and Smiljanić et al. [40] found through research that the crystallization of foam glass would lead to an increase in thermal conductivity. Therefore, in order to improve the thermal insulation of borosilicate foam glass, the crystal phase should be reduced as much as possible.

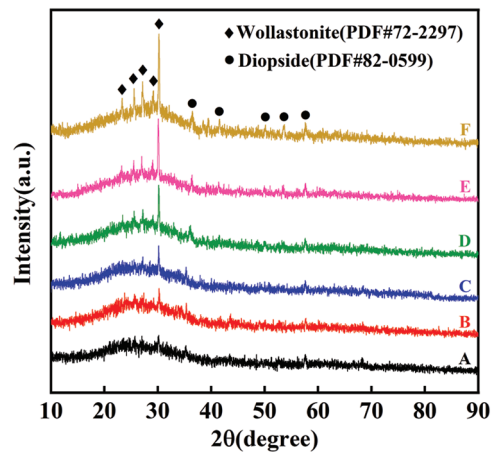


**Figure 6:** X-ray diffraction patterns of borosilicate foam glass

The bulk density of borosilicate foam glass samples decreased from 0.5012 to 0.2060  $\text{g}/\text{cm}^3$ , while the total porosity increased from 78.57% to 90.71% (Fig. 7a). There is a negative correlation between bulk density and total porosity. With the decrease of quartz content and increase of borax content, the viscosity of borosilicate parent glass decreases (Fig. 3b), which leads to the gas generated by the decomposition of the foaming agent expanding more easily in the glass melt.

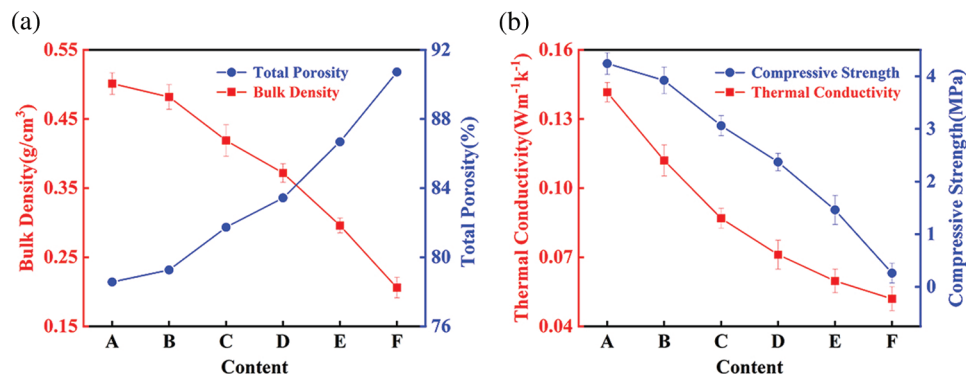


**Figure 7:** Properties of borosilicate foam glass: (a) bulk density and total porosity; (b) compressive strength and thermal conductivity

Heat transfer in foam glass occurs by conduction through the glass phase and gas phase, wherein the gas phase heat transfer includes heat transfer of gas itself, convective heat transfer, and radiation heat transfer [42]. The thermal conductivity of the glass phase heat transfer is much larger than that of the gas phase. It can be basically considered that the heat transfer of foam glass is mainly conducted by glass phase structures such as pore walls, so the thermal conductivity is inversely proportional to pore size and total

porosity. The experimental results conform to this rule (Fig. 7b). In addition, it can be found that the decreasing trend of thermal conductivity is slowing down. On the one hand, as the pore size increases, convective heat transfer in the gas phase increases [28]. On the other hand, as the crystalline phase in the glass phase increases (Fig. 6), the thermal conductivity of the glass phase increases [38,39]. The above two reasons have a negative effect on the reduction of thermal conductivity.

Fig. 7b plots a decrease in the compressive strength (blue line) of borosilicate foam glass samples, showing a trend opposite to total porosity. The compressive strength of the six samples is 4.24, 3.92, 3.06, 2.37, 1.46, and 0.26 MPa, respectively. As the content of quartz decreased from 30 to 17.5 wt.%, and the content of borax increased from 5 to 17.5 wt.%, the compressive strength decreased slightly. While the content of quartz continued to decrease and the content of borax continued to increase, the rate of decrease in compressive strength increased significantly. According to the change of high-temperature viscosity of borosilicate parent glass (Fig. 3b), when the content of quartz is lower than 17.5 wt.% and the content of borax is higher than 17.5 wt.%, the high-temperature viscosity is greatly reduced, and the foaming degree is aggravated, resulting in a rapid decrease in compressive strength of borosilicate foam glass.

The stress-strain curve of the six samples is shown in Fig. 8, and the curves can be roughly divided into three parts:

(1) Linear elastic region: In this stage, the stress and strain are almost proportional until the stress increases to the yield strength ( $\sigma_s$ ). Under the action of load, the whole sample deforms elastically. If unloaded at this stage, the borosilicate foam glass is basically not permanently deformed. (2) Yield platform: When the stress exceeds the yield strength, the strain increases while the stress no longer increases linearly with the strain and fluctuates up and down within a certain range. The stress fluctuation shown in the platform region corresponds to the fracture of each pore wall, and the area enclosed below the platform region represents the energy absorbed by the unit volume of borosilicate foam glass. (3) Densification zone: As the load continues to compress, the pore structure of the sample is completely destroyed so that the glass phase is compacted. The stress rises rapidly with the strain until the sample breaks, and the stress reaches the ultimate strength, which is borosilicate foam glass's compressive strength ( $\sigma_{bc}$ ).

As the content of quartz decreases and the content of borax increases, the foaming degree of borosilicate foam glass gradually increases. This results in an increase of porosity and pore size and a reduction of glass phase pore wall under load. Therefore, the compressive strength and yield strength of the samples decrease gradually. Meanwhile, the yield platform shortens, and the range of stress fluctuation decreases. It is worth noting that the size of the pores is too large, and the amount of pore walls is too small when the content of quartz is 7 wt.% and the content of borax is 28 wt.%. Therefore, in the process of bearing the load, sample F has already broken in the yield stage before the densification stage. Moreover, its yield strength, which is the maximum stress value, is taken as the compressive strength.

### 3.3 Orthogonal Test Results

According to the previous results, the borosilicate foam glass sample D, which was prepared by adding 17.5 wt.% quartz and 17.5 wt.% borax has better comprehensive performance, whose pore distribution is uniform, mean pore size is 1.93 mm, total porosity is 83.44%, thermal conductivity is 0.0711 W/(m·K), and compressive strength is 2.37 MPa. Therefore, this ratio is selected for the orthogonal test. Results of the orthogonal test are shown in Table 5, and results of the range analysis are shown in Table 6.

Fig. 9 shows the optical photos of the samples in the orthogonal test. As the increases of foaming agent content, the gas generated by its decomposition at high-temperature increases, resulting in an increase of gas pressure inside the bubbles, making the bubbles more likely to expand and the pore size to increase. The bubbles break through the pore walls to form connected pores when the foaming agent content increases further (Fig. 9h). As the foaming temperature increases, the viscosity of glass melt decreases (Fig. 3b)

while the decomposition of the foaming agent intensifies, the foaming is gradually sufficient and the pore size increases. The expansion of bubbles is insufficient when the holding time is short, resulting in small pore size and uneven distribution of pores (Fig. 9e). With the holding time extended to 45 min, the bubbles continue to expand and break through the pore wall, causing the gas to escape from the melt, which reduces the pore's size and leads to the connection and collapse of pores (Fig. 9c).

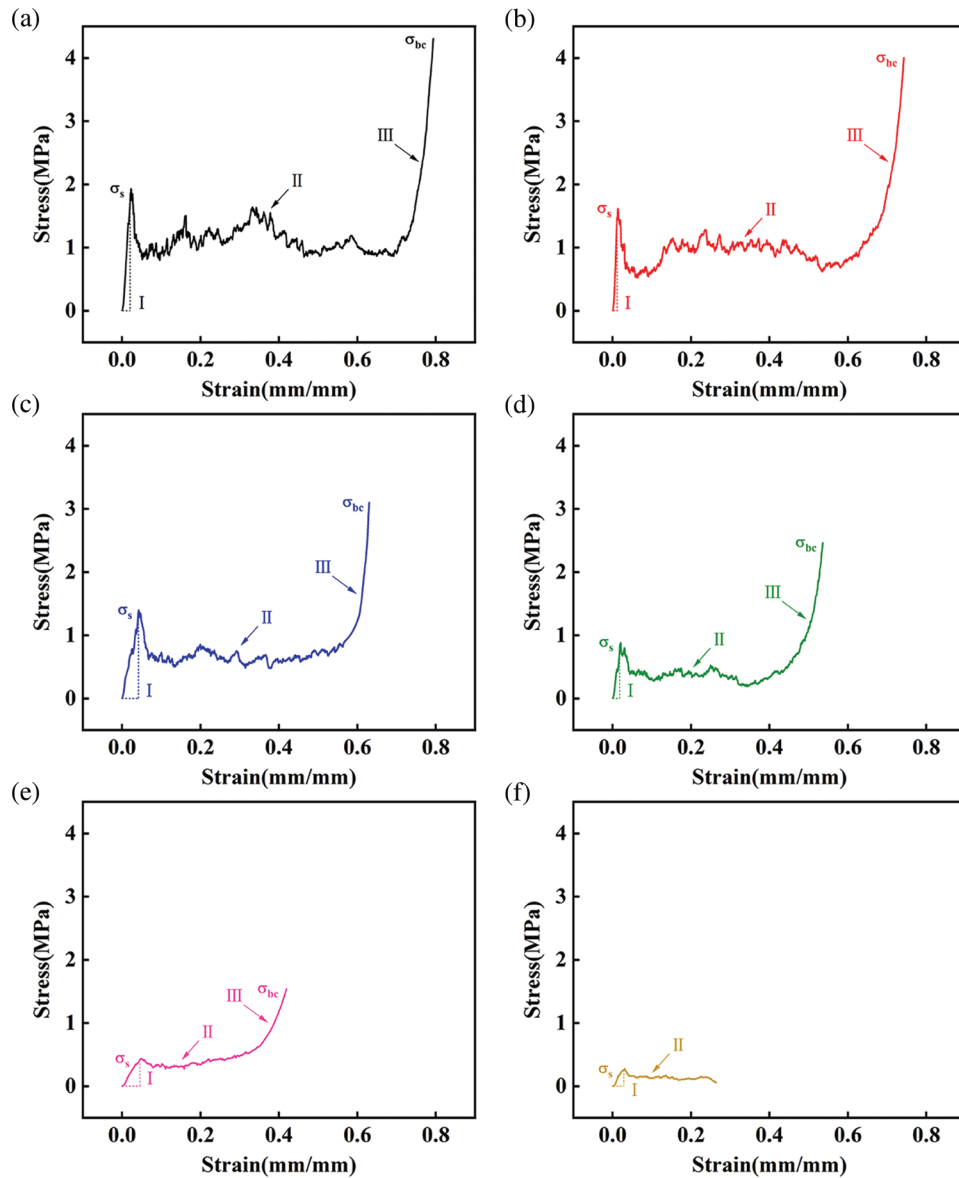


**Figure 8:** Stress-strain curve of borosilicate foam glass

**Table 5:** Orthogonal test results<sup>a</sup>

Sample	W (%)	X (%)	Y (°C)	Z (min)	Mean pore size (mm)	Water absorption (%)	$\lambda$ [W/(m·K)]	$\sigma$ (Mpa)
1	1(1)	1(1)	1(750)	1(15)	0.33	5.01	0.1121	4.22
2	1(1)	2(3)	2(800)	2(30)	1.48	8.34	0.0754	2.63
3	1(1)	3(5)	3(850)	3(45)	1.61	12.87	0.0648	1.45
4	2(3)	1(1)	2(800)	3(45)	1.39	9.48	0.0743	2.23
5	2(3)	2(3)	3(850)	1(15)	1.42	8.81	0.0602	1.74
6	2(3)	3(5)	1(750)	2(30)	0.73	7.86	0.0872	3.86
7	3(5)	1(1)	3(850)	2(30)	2.06	11.80	0.0537	1.38
8	3(5)	2(3)	1(750)	3(45)	0.66	9.29	0.0955	3.42
9	3(5)	3(5)	2(800)	1(15)	1.34	10.41	0.0769	2.16

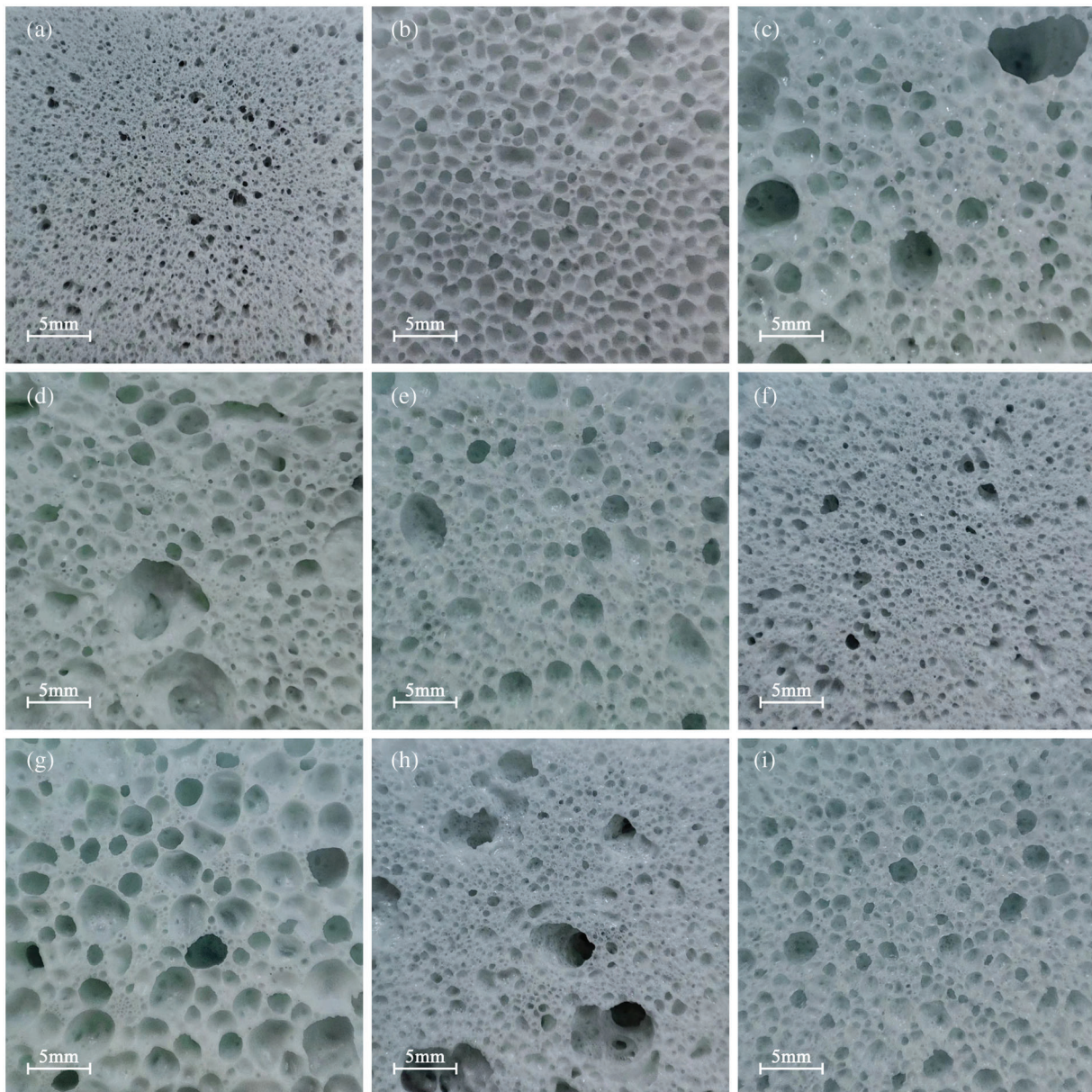
Note: <sup>a</sup> $\lambda$  is thermal conductivity.  $\sigma$  is compressive strength.

**Table 6:** Range analysis of orthogonal test results

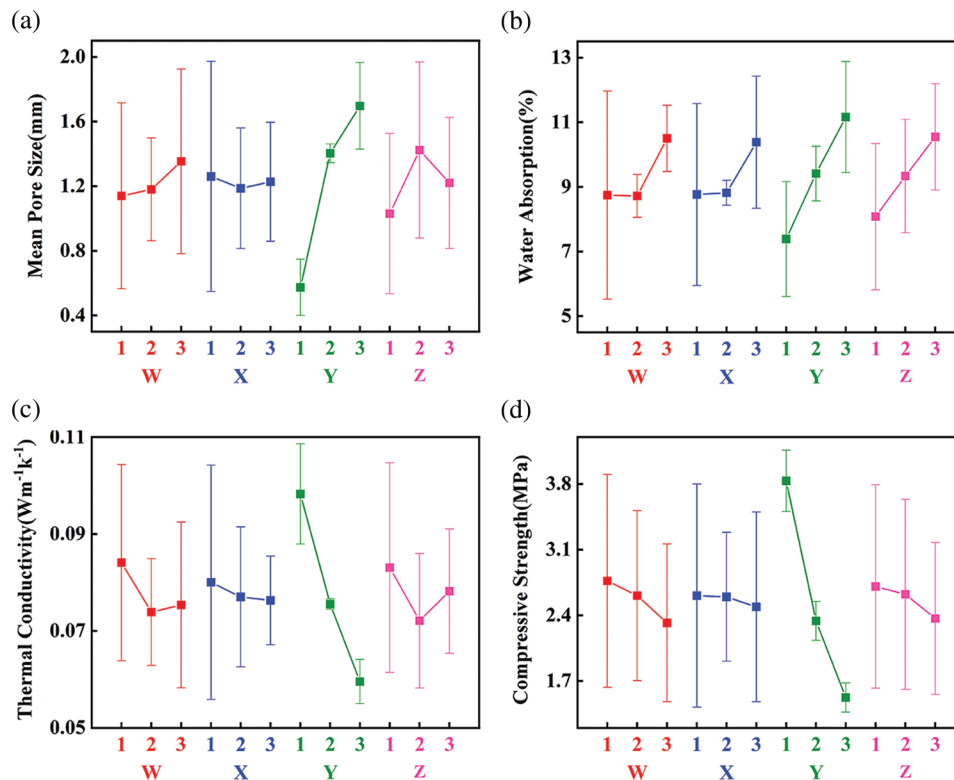
Index		$k1_j$	$k2_j$	$k3_j$	$R_j$
Mean pore size (mm)	W	1.1400	1.1800	1.3533	0.2133
	X	1.2600	1.1867	1.2267	0.0733
	Y	0.5733	1.4033	1.6967	1.1233
	Z	1.0300	1.4233	1.2200	0.3933
Water absorption (%)	W	8.74	8.72	10.50	1.78
	X	8.76	8.82	10.38	1.62
	Y	7.39	9.41	11.16	3.77
	Z	8.08	9.33	10.55	2.47
$\lambda$ [W/(m·K)]	W	0.0841	0.0739	0.0754	0.0102
	X	0.0800	0.0770	0.0763	0.0037
	Y	0.0983	0.0755	0.0596	0.0387
	Z	0.0831	0.0721	0.0782	0.0110
$\sigma$ (Mpa)	W	2.7667	2.6100	2.3200	0.4467
	X	2.6100	2.5967	2.4900	0.0133
	Y	3.8333	2.3400	1.5233	2.3100
	Z	2.7067	2.6233	2.3667	0.3400

Fig. 10 is based on  $k_j$  value in Table 6. Among them,  $k_j$  is the arithmetic mean of the test results under different indexes and levels. It can be seen that the foaming temperature manifests the most significant effect on various properties because the pore size changes greatly with the foaming temperature (Fig. 10a). The effect of flux agent content on various properties is small. However, too much flux agent content would increase the water absorption of the sample. The increase in water absorption is caused by the connection and collapse of pores, so excessive foaming agent content and too long holding time also lead to the increase in water absorption of the samples (Fig. 10b). The connection and collapse of the pores increase

the convective heat transfer of the gas phase, which leads to an increase in thermal conductivity (Fig. 10c). In addition, the connection and collapse of pores would reduce the uniformity of pore structure, resulting in a decrease in the compressive strength (Fig. 10d). Therefore, appropriate foaming agent content, flux agent content, and holding time are conducive to preparing borosilicate foam glass with excellent comprehensive properties.



**Figure 9:** Optical photos of borosilicate foam glass in the orthogonal test ((a)–(i) are the borosilicate foam glass 1–9 in the orthogonal test, respectively)



**Figure 10:** Curve of range analysis of orthogonal test results

#### 4 Conclusion

- (1) By adding quartz, borax, and other raw materials to the recycled soda lime waste glass to melt the special borosilicate parent glass, and then adding 3 wt.%  $CaCO_3$  as foaming agent and 3 wt.%  $Na_2CO_3$  as flux agent, foaming at  $800^\circ C$  for 30 min can prepare borosilicate foam glass with uniform pore structure.
- (2) With the decrease of quartz content and increase of borax content, the pore size and total porosity of borosilicate foam glass increase gradually, while the compressive strength and thermal conductivity decrease. When the quartz content is 17.5 wt.%, and borax content is 17.5 wt.%, the comprehensive performance of the borosilicate foam glass prepared is outstanding, whose bulk density is  $0.3718 \text{ g/cm}^3$ , total porosity is 83.44%, thermal conductivity is  $0.0711 \text{ W/(m}\cdot\text{K)}$ , and compressive strength is 2.37 MPa.
- (3) According to the analysis results of the orthogonal test, the foaming temperature has a significant effect on the pore structure and properties of borosilicate foam glass. Appropriate foaming agent content, flux agent content, and holding time can reduce the collapse of pores and the appearance of connected pores, thereby improving the thermal insulation and mechanical strength of borosilicate foam glass.

**Acknowledgement:** We thank Assistant Professor Linfeng Ding (Donghua University) for support of High-Temperature Viscosity Measurement. We thank Master Shun Wang for her help of FT-IR Testing. We also thank Master Guoqiang Wu for SEM Micrographs.

**Funding Statement:** This work was supported by the Shanghai Municipal Natural Science Foundation, China (Granted No. [19ZR1418500]).

**Conflicts of Interest:** The authors declare that they have no conflicts of interest to report regarding the present study.

## References

1. König, J., Petersen, R. R., Iversen, N., Yue, Y. (2018). Suppressing the effect of cullet composition on the formation and properties of foamed glass. *Ceramics International*, 44(10), 11143–11150. DOI 10.1016/j.ceramint.2018.03.130.
2. Oo D'Amore, G. K., Caniato, M., Travan, A., Turco, G., Marsich, L. et al. (2017). Innovative thermal and acoustic insulation foam from recycled waste glass powder. *Journal of Cleaner Production*, 165, 1306–1315. DOI 10.1016/j.jclepro.2017.07.214.
3. König, J., Lopez-Gill, A., Cimavilla-Roman, P., Rodriguez-Perez, M. A., Petersen, R. R. et al. (2020). Synthesis and properties of open- and closed-porous foamed glass with a low density. *Construction and Building Materials*, 247, 118574. DOI 10.1016/j.conbuildmat.2020.118574.
4. Siddika, A., Hajimohammadi, A., Sahajwalla, V. (2022). Powder sintering and gel casting methods in making glass foam using waste glass: A review on parameters, performance, and challenges. *Ceramics International*, 48(2), 1494–1511. DOI 10.1016/j.ceramint.2021.10.066.
5. König, J., Petersen, R. R., Yue, Y. (2016). Influence of the glass particle size on the foaming process and physical characteristics of foam glasses. *Journal of Non-Crystalline Solids*, 447, 190–197. DOI 10.1016/j.jnoncrysol.2016.05.021.
6. Ewais, E. M. M., Attia, M. A. A., El-Amir, A. A. M., Elshenway, A. M. H., Fend, T. (2018). Optimal conditions and significant factors for fabrication of soda lime glass foam from industrial waste using nano AlN. *Journal of Alloys and Compounds*, 747, 408–415. DOI 10.1016/j.jallcom.2018.03.039.
7. Erasmus, E. P., Sule, R., Johnson, O. T., Massera, J., Sigalas, I. (2018). In vitro evaluation of porous borosilicate, borophosphate and phosphate bioactive glasses scaffolds fabricated using foaming agent for bone regeneration. *Scientific Reports*, 8(1), 3699. DOI 10.1038/s41598-018-22032-2.
8. Llaudis, A. S., Tari, M. J. O., Ten, F. J. G., Bernardo, E., Colombo, P. (2009). Foaming of flat glass cullet using Si<sub>3</sub>N<sub>4</sub> and MnO<sub>2</sub> powders. *Ceramics International*, 35(5), 1953–1959. DOI 10.1016/j.ceramint.2008.10.022.
9. Vancea, C., Lazău, I. (2014). Glass foam from window panes and bottle glass wastes. *Open Chemistry*, 12(7), 804–811. DOI 10.2478/s11532-014-0510-x.
10. Owoeye, S. S., Matthew, G. O., Oviemhanda, F. O., Tunmilayo, S. O. (2020). Preparation and characterization of foam glass from waste container glasses and water glass for application in thermal insulations. *Ceramics International*, 46(8), 11770–11775. DOI 10.1016/j.ceramint.2020.01.211.
11. Sooksaen, P., Sudyod, N., Thongtha, N., Somsomboonphol, R. (2019). Fabrication of lightweight foam glasses for thermal insulation applications. *Materials Today: Proceedings*, 17, 1823–1830.
12. da Silva, R. C., Kubaski, E. T., Tenório-Neto, E. T., Lima-Tenório, M. K., Tebcherani, S. M. (2019). Foam glass using sodium hydroxide as foaming agent: Study on the reaction mechanism in soda-lime glass matrix. *Journal of Non-Crystalline Solids*, 511, 177–182. DOI 10.1016/j.jnoncrysol.2019.02.003.
13. Abdollahi, S., Yekta, B. E. (2020). Prediction of foaming temperature of glass in the presence of various oxidizers via thermodynamics route. *Ceramics International*, 46(16), 25626–25632. DOI 10.1016/j.ceramint.2020.07.037.
14. Østergaard, M. B., Petersen, R. R., König, J., Bockowski, M., Yue, Y. (2019). Impact of gas composition on thermal conductivity of glass foams prepared via high-pressure sintering. *Journal of Non-Crystalline Solids: X*, 1, 100014. DOI 10.1016/j.nocx.2019.100014.
15. Constantin, N., Ioana, A., Tufeanu, D., Paunescu, L., Marcu, D. F. et al. (2021). Separation and recycling of cathode ray tube (CRT) glass waste by foaming in microwave field. *Revista Romana de Materiale-Romanian Journal of Materials*, 51(3), 378–385.
16. Cengizler, H., Koç, M., Şan, O. (2021). Production of ceramic glass foam of low thermal conductivity by a simple method entirely from fly ash. *Ceramics International*, 47(20), 28460–28470. DOI 10.1016/j.ceramint.2021.06.265.
17. Song, H., Chai, C., Zhao, Z., Wei, L., Wu, H. et al. (2021). Experimental study on foam glass prepared by hydrothermal hot pressing-calcination technique using waste glass and fly ash. *Ceramics International*, 47(20), 28603–28613. DOI 10.1016/j.ceramint.2021.07.019.

18. Xi, C., Zhou, J., Zheng, F., Gao, J., Hu, P. et al. (2020). Conversion of extracted titanium tailing and waste glass to value-added porous glass ceramic with improved performances. *Journal of Environmental Management*, 261, 110197. DOI 10.1016/j.jenvman.2020.110197.
19. Zhang, C., Wang, X., Zhu, H., Wu, Q., Hu, Z. et al. (2020). Preparation and properties of foam ceramic from nickel slag and waste glass powder. *Ceramics International*, 46(15), 23623–23628. DOI 10.1016/j.ceramint.2020.06.134.
20. Cheng, H., Li, X., Zhang, J., Wei, B. (2007). Study on borosilicate foam glass. *Bulletin of the Chinese Ceramic Society*, 26(2), 264–267.
21. Wang, M., Bu, F., Zhou, C., Zhou, Q., Wei, T. et al. (2020). Bonding performance and mechanism of a heat-resistant composite precursor adhesive (RT-1000°C) for TC<sub>4</sub> titanium alloy. *Journal of Micromechanics and Molecular Physics*, 5(4), 2050016. DOI 10.1142/S2424913020500162.
22. Wang, M., Liu, J., Chen, Z., Hu, X., Zhai, W. et al. (2022). Joining zirconia with nickel-based superalloys for extreme applications by using a pressure-free high-temperature resistant adhesive. *Ceramics International*, 48(6), 8025–8030. DOI 10.1016/j.ceramint.2021.12.002.
23. Zhai, C., Li, Z., Zhu, Y., Zhang, J., Wang, X. et al. (2014). Effects of Sb<sub>2</sub>O<sub>3</sub> on the mechanical properties of the borosilicate foam glasses sintered at low temperature. *Advances in Materials Science and Engineering*, 2014, 1–6. DOI 10.1155/2014/703194.
24. Zhai, C., Zhong, Y., Liu, J., Zhang, J., Zhu, Y. et al. (2022). Customizing the properties of borosilicate foam glasses via additions under low sintering temperatures with insights from molecular dynamics simulations. *Journal of Non-Crystalline Solids*, 576, 121273. DOI 10.1016/j.jnoncrysol.2021.121273.
25. Zhai, C., Zhong, Y., Zhang, J., Wang, M., Yu, Y. et al. (2022). Enhancing the foaming effects and mechanical strength of foam glasses sintered at low temperatures. *Journal of Physics and Chemistry of Solids*, 165, 110698. DOI 10.1016/j.jpics.2022.110698.
26. Taurino, R., Lancellotti, I., Barbieri, L., Leonelli, C. (2014). Glass-ceramic foams from borosilicate glass waste. *International Journal of Applied Glass Science*, 5(2), 136–145. DOI 10.1111/ijag.12069.
27. Chinnam, R. K., Molinaro, S., Bernardo, E., Boccaccini, A. R. (2014). Borosilicate glass foams from glass packaging residues. *Ceramics for Environmental and Energy Applications II*, 246(164), 203–210.
28. Salleh, Z., Islam, M. M., Epaarachchi, J. A. (2018). Thermal expansion properties of fused borosilicate syntactic foams. *Nano Hybrids and Composites*, 23, 39–45. DOI 10.4028/www.scientific.net/NHC.23.39.
29. Salleh, Z., Islam, M. M., Epaarachchi, J. A., Khan, M. T. I. (2019). Thermo-mechanical properties of fused borosilicate syntactic foams. *Journal of Mechanical Engineering and Sciences*, 13(2), 4898–4910. DOI 10.15282/jmes.13.2.2019.10.0407.
30. Liu, Y., Xie, J., Hao, P., Shi, Y., Xu, Y. et al. (2021). Study on factors affecting properties of foam glass made from waste glass. *Journal of Renewable Materials*, 9(2), 237–253. DOI 10.32604/jrm.2021.012228.
31. Tang, Y., Jiang, Z., Song, X. (1989). NMR, IR and Raman spectra study of the structure of borate and borosilicate glasses. *Journal of Non-Crystalline Solids*, 112(1), 131–135.
32. Verhoef, A. H., den Hartog, H. W. (1995). Structure and dynamics of alkali borate glasses: A molecular dynamics study. *Journal of Non-Crystalline Solids*, 182(3), 235–247. DOI 10.1016/0022-3093(94)00554-0.
33. Liu, S., Zhao, G., Ying, H., Wang, J., Han, G. (2008). Effects of mixed alkaline earth oxides additive on crystallization and structural changes in borosilicate glasses. *Journal of Non-Crystalline Solids*, 354(10–11), 956–961. DOI 10.1016/j.jnoncrysol.2007.08.027.
34. Wan, J., Cheng, J., Lu, P. (2008). The coordination state of B and Al of borosilicate glass by IR spectra. *Journal of Wuhan University of Technology-Materials Science Edition*, 23(3), 419–421. DOI 10.1007/s11595-007-3419-9.
35. Fábíán, M., Sváb, E., Proffen, T., Veress, E. (2008). Structure study of multi-component borosilicate glasses from high-Q neutron diffraction measurement and RMC modeling. *Journal of Non-Crystalline Solids*, 354(28), 3299–3307. DOI 10.1016/j.jnoncrysol.2008.01.024.
36. Stebbins, J. F., Sen, S. (1998). Microscopic dynamics and viscous flow in a borosilicate glass-forming liquid. *Journal of Non-Crystalline Solids*, 224(1), 80–85. DOI 10.1016/S0022-3093(97)00456-0.

37. Ding, L., Thieme, M., Demouchy, S., Kunisch, C., Kaus, B. J. P. (2018). Effect of pressure and temperature on viscosity of a borosilicate glass. *Journal of the American Ceramic Society*, 101(9), 3936–3946. DOI 10.1111/jace.15588.
38. Petersen, R. R., König, J., Yue, Y. (2017). The viscosity window of the silicate glass foam production. *Journal of Non-Crystalline Solids*, 456, 49–54. DOI 10.1016/j.jnoncrysol.2016.10.041.
39. Méar, F., Yot, P., Ribes, M. (2006). Effects of temperature, reaction time and reducing agent content on the synthesis of macroporous foam glasses from waste funnel glasses. *Materials Letters*, 60(7), 929–934. DOI 10.1016/j.matlet.2005.10.046.
40. Smiljanić, S., Hribar, U., Spreitzer, M., König, J. (2021). Influence of additives on the crystallization and thermal conductivity of container glass cullet for foamed glass preparation. *Ceramics International*, 47(23), 32867–32873. DOI 10.1016/j.ceramint.2021.08.183.
41. Østergaard, M. B., Petersen, R. R., König, J., Johra, H., Yue, Y. (2017). Influence of foaming agents on solid thermal conductivity of foam glasses prepared from CRT panel glass. *Journal of Non-Crystalline Solids*, 465, 59–64. DOI 10.1016/j.jnoncrysol.2017.03.035.
42. Cimavilla-Román, P., Villafañe-Calvo, J., López-Gil, A., König, J., Rodríguez-Perez, M. Á. (2021). Modelling of the mechanisms of heat transfer in recycled glass foams. *Construction and Building Materials*, 274, 122000. DOI 10.1016/j.conbuildmat.2020.122000.